BIOCHEMISTRY
including biophysical chemistry & molecular biology
Article

Biochemistry **2009,** *48,* 5149–5158 5149
DOI: 10.1021/bi900257m

Using Substrate Specificity of Antiplasmin-Cleaving Enzyme for Fibroblast Activation Protein Inhibitor Design†

Kyung N. Lee,*,‡ Kenneth W. Jackson,‡ Simon Terzyan,§ Victoria J. Christiansen,‡ and Patrick A. McKee‡

‡*William K. Warren Research Center and Department of Medicine, University of Oklahoma Health Sciences Center, Oklahoma City, Oklahoma 73126, and* §*Oklahoma Medical Research Foundation, Oklahoma City, Oklahoma 73104*

Received February 16, 2009; Revised Manuscript Received April 28, 2009

ABSTRACT: Circulating antiplasmin-cleaving enzyme (APCE), a prolyl-specific serine proteinase, is essentially identical to membrane-inserted fibroblast activation protein (FAP) that is transiently expressed during epithelial-derived cancer growth. Human precursive α_2-antiplasmin (Met-α_2AP), the only known physiologic substrate for APCE, is cleaved N-terminally to Asn-α_2AP that is rapidly cross-linked to fibrin and protects it from digestion by plasmin. Identifying a specific inhibitor of APCE/FAP continues to be intensely pursued. Recombinant FAP cleavage of peptide libraries of short amino acid sequences surrounding the scissile bond, -Pro^{12}-Asn^{13}-, indicated that P2 Gly and P1 Pro are required, just as we found for APCE. We examined cleavage of P4−P4′ peptides, using 19 amino acid substitutions at each position and selected ones in P8−P5. K_m values determined for peptide substrates showed that P7 Arg has the highest affinity for APCE. Peptide cleavage rate increased with Arg in P6 rather than P5 or native P7. Placing Arg in P4 or P8 reduced cleavage rates dramatically. Cleavage of substrates with extended peptide sequences before or after the scissile bond showed endopeptidase to be superior to dipeptidase activity for APCE. A substrate analogue inhibitor, Phe-Arg-(8-amino-3,6-dioxaoctanoic acid)-Gly-[*r*]-fluoropyrrolidide, inhibited APCE with a K_i of 54 μM but not dipeptidyl peptidase IV even at 2 mM. The inhibitor also blocked cleavage of Met-α_2AP with an IC_{50} of 91 μM. Replacing Arg with Gly at the same distance from fluoropyrrolidide as P7 Arg is from P1 Pro reduced its inhibition of APCE ~10-fold. Results indicate that Arg at P5, P6, or P7 distances from P1 enhances affinity and efficiency of substrates or inhibitors toward APCE or FAP.

Human α_2-antiplasmin (α_2AP),[1] the primary inhibitor of plasmin, is secreted from liver cells as a single-chain glycoprotein of 464 amino acid residues with an N-terminal methionine (Met-α_2AP). An N-terminal 12-residue peptide is cleaved from Met-α_2AP between Pro^{12} and Asn^{13} by circulating antiplasmin-cleaving enzyme (APCE), a prolyl-specific serine proteinase, to yield the derivative, Asn-α_2AP (*1*). To date, Met-α_2AP is the only defined physiologic substrate for APCE. Met-α_2AP is found in plasma in two polymorphic forms, having either Arg (R) or Trp (W) as its sixth residue, i.e., R6 or W6, the former being cleaved by APCE ~8-fold faster than the latter to yield Asn-α_2AP (*2*). During clot formation, Asn-α_2AP becomes cross-linked to fibrin by activated clotting factor XIII ~13-fold faster than Met-α_2AP (R6) or Met-α_2AP(W6), and as reported by us, clot lysis rates decrease in direct proportion to the plasma ratio of Asn-α_2AP/Met-α_2AP (*1*, *3*). This prompted the hypothesis that an enhanced endogenous fibrinolytic activity might be accomplished by increasing Met-α_2AP/Asn-α_2AP ratios through inhibition of APCE (*2*).

APCE is a soluble isoform or derivative of fibroblast activation protein (FAP) (*4*), the latter being a type II integral membrane protein, which is predicted to have its first six N-terminal residues within fibroblast cytoplasm, followed by a 20-residue transmembrane domain and then a 734-residue extracellular C-terminal catalytic domain (*5*, *6*). Recombinant FAP, like APCE, is also a prolyl-specific enzyme that exhibits both endopeptidase and dipeptidyl peptidase activities (*7*). FAP is expressed by activated fibroblasts and is believed to proteolytically remodel the extracellular matrix during embryogenesis, wound healing, and expansion of epithelial-derived cancers (e.g., breast, lung, prostate, pancreas, colon, gastric). FAP is not expressed by normal tissues or benign tumors (*6*, *8*−*17*). A few reports have shown that human parenchymal carcinoma cells may also contain cytosolic and membrane forms of FAP (*14*, *16*). In an animal model, transfected HK293 cells that expressed FAP promoted tumor growth (*18*). FAP has also been noted in other diseases characterized by marked fibroblast proliferation and abnormal tissue growth. In hepatic cirrhosis, FAP expression occurs exclusively on activated hepatic stellate

†This work was supported by the W. K. Warren Medical Research Center, the National Institutes of Health (HL072995), the Department of Defense, and the Oklahoma Center for the Advancement of Science and Technology.

*To whom correspondence should be addressed. Phone (405) 271-3920. Fax: (405) 271-3229. E-mail: kyung-lee@ouhsc.edu.

[1]Abbreviations: AMC, amido-4-methylcoumarin; APCE, antiplasmin-cleaving enzyme; α_2AP, α_2-antiplasmin; DPPIV, dipeptidyl peptidase IV; FAP, fibroblast activation protein; HATU, 2-(7-aza-1*H*-benzotriazol-1-yl)-1,1,3,3-tetramethyluronium hexafluorophosphate; HBTU, 2-(1*H*-benzotriazol-1-yl)-1,1,3,3-tetramethyluronium hexafluorophosphate; HOBT, 1-hydroxybenzotriazole; K_i, inhibition constant.

Published on Web 04/29/2009

cells and myofibroblasts and correlates strongly with severity of fibrosis (*19*). In osteoarthritis, FAP is significantly higher on chondrocyte membranes and cartilage than in normal counterpart tissue (*20*). Finally, high FAP expression may play a role in the relentless advancement of idiopathic pulmonary fibrosis (*21*). The suspicion that FAP relates to progression and severity of several major chronic diseases has stimulated efforts to develop an inhibitor of its proteinase activity.

Stable and specific inhibitors are needed to decipher the relationship between APCE activity and fibrin clot lysis or FAP activity and neoplasm growth. With the objective of developing specific inhibitors of APCE, we now report complete cleavage rate analyses of synthetic peptide libraries, modeled on the P4−P4′ sequence spanning the cleavage site in Met-α_2AP to identify preferred or requisite residues. Our results also provide insights about the impact of the P7 functional single nucleotide polymorphism on cleavage of the Met-α_2AP scissile bond (Pro^{12}-Asn^{13}) by APCE (*2*). Peptide motifs potentially useful in the design of selective inhibitors of both APCE and FAP are shown not only to significantly inhibit cleavage of synthetic fluorescent substrates but also, for the first time, to inhibit cleavage of the natural human substrate, Met-α_2AP.

EXPERIMENTAL PROCEDURES

Materials. Gly-Pro-7-amido-4-methylcoumarin (Gly-Pro-AMC) and benzyloxycarbonyl- (Z-) Gly-Pro-AMC were from Sigma and Bachem, respectively. Fmoc-pipecolinic acid and Fmoc-(3*S*)-1,2,3,4-tetrahydroisoquinoline-3-carboxylic acid (tic) were from Advanced Chemtech; pyrrolidine and piperidine were from Aldrich. MEPLGRQLTSGP-AMC, MEPLGWQLTSGP-AMC, peptide substrate analogue inhibitors, and peptide libraries were synthesized in the Molecular Biology-Proteomics Facility, University of Oklahoma Health Sciences Center. Met-α_2AP(R6) and APCE were purified as previously described from fresh frozen human plasma purchased from the Sylvan Goldman Blood Institute, Oklahoma City, OK (*4*).

Synthesis of Inhibitors. Inhibitors **1**−**4** and **11** listed in Table 2 were prepared according to the Fmoc synthesis procedure utilizing the HBTU/HOBT activation method [the activation reaction consisted of 3.3 equiv of HBTU (2-(1*H*-benzotriazol-1-yl)-1,1,3,3-tetramethyluronium hexafluorophosphate), 3.3 equiv of HOBT (1-hydroxybenzotriazole), 6.6 equiv of diisopropylethylamine, 3.3 equiv of protected amino acid, and 1.0 equiv of amino acid or peptide linked to the synthesis solid support]. All reactions were carried out in *N*-methylpyrrolidone. The syntheses were done by solid-phase methods employing 4-alkylbenzyloxy alcohol resins for inhibitors **1**−**4** and Rink 4-methylbenzhydrylamine resin for inhibitor **11**. Inhibitors **5**−**10** were partially synthesized, including all but the C-terminal structure, utilizing the above methods on glycine-2-chlorotrityl resins on all except inhibitor **7**, where 8-amino-3,6-dioxaoctanoic acid-2-chlorotrityl resin was used. For inhibitors **5**−**10**, chemically protected peptides were released from the synthesis resin by treatment with 3% trifluoroacetic acid in dichloromethane. The protected peptides were then purified by reversed-phase HPLC. Inhibitor **5**−**7** precursors were prepared by this method, and then each protected peptide's free carboxyl terminus was linked to a 5-fold excess of pyrrolidine (inhibitors **5**−**7**), fluoropyrrolidine (inhibitors **8** and **9**), or piperidine (inhibitor **10**) by in-solution reaction utilizing the HATU/DIEA linkage reaction in dimethylformamide. The HATU/DIEA linkage reaction mixture contained 1.2 equiv of HATU (2-(7-aza-1*H*-benzotriazol-1-yl)-1,1,3,3-tetramethyluronium hexafluorophosphate), 2.4 equiv of diisopropylethylamine, and 1.0 equiv of protected peptide. The reaction products were chemically deprotected by treatment with 90% trifluoroacetic acid, 5% triisopropylsilane, and 5% water and then dried. Finally, each inhibitor was purified by reversed-phase HPLC and analyzed by electrospray mass spectrometry.

Enzyme Assays. APCE or DPPIV was incubated in 25 mM sodium phosphate buffer, pH 7.5, containing 1.0 mM EDTA and 4% methanol in a total volume of 200 μL for 20 min at 22 °C, using fluorescent substrates MEPLGRQLTSGP-AMC (5−160 μM), MEPLGWQLTSGP-AMC (10−400 μM), Z-Gly-Pro-AMC (10−500 μM), or Gly-Pro-AMC (50−2500 μM). Fluorescence was monitored with time at excitation and emission wavelengths of 360 and 460 nm using a black-sided, 96-well plate in a BIO-TEK FL600 fluorescence plate reader. For standard curves, dilutions of AMC (7-amido-4-methylcoumarin) were prepared in the same assay buffer, and corresponding fluorescence was measured. The substrates in five different concentrations were mixed with four different concentrations of inhibitors around the expected K_i values; the enzyme was added and enzymatically released AMC fluorescence was recorded. Competitive inhibition was established by Lineweaver−Burk plot. Therefore, enzyme kinetic parameters were computed by fitting data to the following equation, employing the program PRISM, GraphPad:

$$v = \frac{V_{max}[S]}{K_m\left(1 + \frac{[I]}{K_i}\right) + [S]}$$

APCE Residue Preferences in P4−P4′ Substrate Peptides. To determine substrate specificity in P4−P4′, peptides were derived from the contiguous sequence of four amino acids on either side of the APCE Pro^{12}-Asn^{13} cleavage site in Met-α_2AP. Eight peptide position libraries were prepared; each library consisted of different peptides with each having a single amino acid position substituted utilizing all native amino acids except Cys. Within each library, the 19 peptides were distributed into three sublibraries with six or seven peptides in each. The peptides in a sublibrary were selected so that the molecular weight differences among them were maximized. Each of the three sublibraries contained a common specific reference peptide. In total, there were 152 peptides with each differing from the others by a single amino acid in the 24 sublibraries representing the eight position libraries. Each sublibrary was incubated with APCE, and relative cleavage rates for each peptide in the mixture were compared.

Reaction mixtures contained APCE at 0.5−2 μg and peptide concentrations of 13.4 μM for each that contained residues from the P-side or 18.6 μM for peptides modeled from P′-side amino acids. Amounts of cleaved peptides were determined at 0.083, 0.167, 0.25, 0.33, 0.50, 0.75, 1.0, 1.5, 3.0, 4.0, 6.0, and 24 h. To buttress conclusions about P4−P4′ substrate specificity from the LC/MS data, only time points below 15% substrate consumption were utilized to ensure cleavage rates remained within a linear range. Cleavage rates of peptide substrates in the P1−P4 sublibraries by APCE were determined by liquid chromatography/mass spectrometry (LC/MS) analysis. Peptide libraries representing residue numbers 6 through 17 (FRQL**TSGP**-NQEQV) of Met-α_2AP(R6) sequence were incubated with APCE; each bold and underlined letter represents the varied amino acid. The FRQL sequence was added to make the

Table 1: Kinetic Values for APCE and DPPIV

substrate	APCE			DPPIV		
	K_m (mM)	k_{cat} (min^{-1})	k_{cat}/K_m (min^{-1}/mM)	K_m (mM)	k_{cat} (min^{-1})	k_{cat}/K_m (min^{-1}/mM)
MEPLGRQLTSGP-AMC	0.021 ± 0.002	70.2 ± 2.3	3.3×10^3	NC[a]		
MEPLGWQLTSGP-AMC	0.070 ± 0.006	55.3 ± 1.5	7.9×10^2	NC		
Z-GP-AMC	0.090 ± 0.009	36.4 ± 1.2	4.0×10^2	NC		
GP-AMC	0.455 ± 0.042	29.1 ± 1.1	6.4×10^1	0.063 ± 0.006	119.1 ± 6.1	1.9×10^3

[a] NC: no cleavage.

N-terminal product larger in molecular weight than the C-terminal product. The N-terminal Phe, not native to Met-α_2AP, was added to enhance binding to the reversed-phase HPLC column.

To determine P1′−P4′ substrate specificity, peptide cleavage rates were analyzed by MALDI-TOF MS. Peptide libraries representing residue numbers 9 through 18 (ATSGP-**NQEQ**VSFR) of Met-α_2AP sequence, with each bold letter representing the varied amino acid, were also incubated with APCE. N-Terminal Ala and C-terminal Phe and Arg were added to improve MALDI-TOF MS analysis.

LC/MS Analysis of Met-α_2AP Hydrolysis by APCE. Met-α_2AP(R6) (13 μg) was incubated with APCE (0.2 μg) and various concentrations of inhibitor in 100 μL of 25 mM sodium phosphate−1.0 mM EDTA buffer, pH 7.5. After incubation for 6 h at 37 °C, an internal standard peptide (FRQLTSG-tic-NQEQV, 0.11 μg) was dissolved in the reaction mixture, and cold acetonitrile (4× sample volume) was added to precipitate proteins. The sample was incubated at −80 °C for 60 min and centrifuged for 10 min at 16000*g* at 4 °C to remove precipitated proteins. The supernatant, which contained the N-terminal 12-residue peptide of Met-α_2AP(R6), was removed, dried by vacuum centrifugation, and dissolved in 5% acetic acid.

Hydrolysis products contained in the supernatant were analyzed by LC/MS, using a Paradigm MS4B HPLC system (Michrom Bioresources) equipped with a reversed-phase column (0.5 mm × 150 mm Magic C18 column with 5 μm particles and 20 nm pores) operated at 20 μL/min. The column was equilibrated with 2% acetonitrile/water containing 0.09% formic acid and 0.01% TFA. Upon sample injection, the solvent composition was increased to 10% acetonitrile, and a linear gradient was applied to 50% acetonitrile over 40 min. Peptides were detected at 215 nm wavelength. The HPLC effluent was connected to an HCTultra ion trap mass spectrometer, Bruker Daltonics, equipped with an electrospray ion source operated in the positive ion mode. Data were collected over an m/z range of 300−1800 amu. Both the internal standard peptide and the peptide product of digestion were located by extracted ion current analysis of data for each peptide over a 1.5 amu window for singly and doubly charged forms of each peptide, based on the peptide's predicted monoisotopic molecular mass. Quantification was performed by summing all detected ions from the total ion chromatogram for all observed charge forms and all isotopic forms detected above background for each peptide ion over a 2 min window beginning when peptide ions were first observed.

Immunoblot Analysis of Met-α_2AP Cleavage by APCE. Reaction mixtures made to contain APCE, Met-α_2AP(R6), and one of the inhibitors from Table 2 were prepared as described above, incubated for 6 h, subjected to SDS−PAGE, and transferred to a nitrocellulose membrane, and Met-α_2AP(R6) was then detected by immunostaining with an antibody specific for its N-terminal sequence and nonreactive with Asn-α_2AP (*1*).

RESULTS

Effects of Met-α_2AP(R6W) Polymorphism on Binding to APCE. Met-α_2AP exists in two polymorphic forms, Met-α_2AP(R6) and Met-α_2AP(W6), and while APCE cleaves the former at Pro^{12}-Asn^{13} ~8-fold faster than the latter to remove the 12-residue N-terminal peptide (*2*); it is unknown if the rate difference is due to variation in APCE binding to the linear peptide sequence or to conformational changes induced within Met-α_2AP by the R6W polymorphism. To clarify this, we synthesized peptides that contained N-terminal amino acids P1−P12, with either R or W at P7, and the C-terminal fluorogenic group, AMC, at P1′, i.e., MEPLGRQLTSGP-AMC or MEPLGWQLTSGP-AMC, and determined kinetic parameters for cleavage of each by APCE (Table 1). Replacement of P7 Arg with Trp caused a 3.5-fold increase in the K_m and a 4.2-fold decrease in k_{cat}/K_m, which supports that the increased rate of APCE cleavage of Met-α_2AP(R6) can be explained in large part by increased affinity between APCE and Met-α_2AP(R6).

Endopeptidase Specificity of APCE. While Arg in P7 conferred more than a 3-fold increase in substrate affinity for APCE (Table 1), it persistently resulted in the Pro^{12}-Asn^{13} scissile bond being cleaved ~8-fold faster (*2*). These observations suggested that a positively charged P7 residue relates to substrate selectivity and might augment approaches for bypassing overlapping interactions with other prolyl-specific serine peptidases. The specific impact of P7 on APCE endopeptidase activity suggested that, like FAP (*22*), this function may prevail over potential dipeptidase properties. Although APCE is known to cleave prolyl peptide (Pro-Xaa) bonds, no direct quantitative study of its dipeptidyl peptidase and endopeptidase activities has been reported. Therefore, two 17-residue peptides surrounding the APCE cleavage site in Met-α_2AP(R6) were synthesized and hydrolyzed with equivalent amounts of APCE. The peptides, MEPLGRQLTSG**P-N**QEQV and G**P-N**QEQVSPLTLLKLGN (scissile bond in bold), were used as the endopeptidase and aminodipeptidase substrates. Figure 1 clearly shows that APCE is preferentially an endopeptidase rather than an aminodipeptidase, with an ~10-fold greater rate of hydrolysis of the internal **-P-N-** bond in the Met-α_2AP(R6) 1−17 native peptide sequence, MEPLGRQLTSG**P-N**QEQV, when compared to cleavage of the **-P-N-** dipeptidyl bond exposed in the Met-α_2AP 11−27 amino acid sequence, G**P-N**QEQVSPLTLLKLGN. That the endopeptidase activity of APCE dominates is further supported by experiments using fluorometric substrates, MEPLGRQLTSGP-AMC, MEPLGWQLTSGP-AMC, Z-GP-AMC, and GP-AMC. Similar to the studies of Aertgeerts et al. (*22*) in which recombinant FAP showed an ~18-fold increase in catalytic efficiency for cleaving

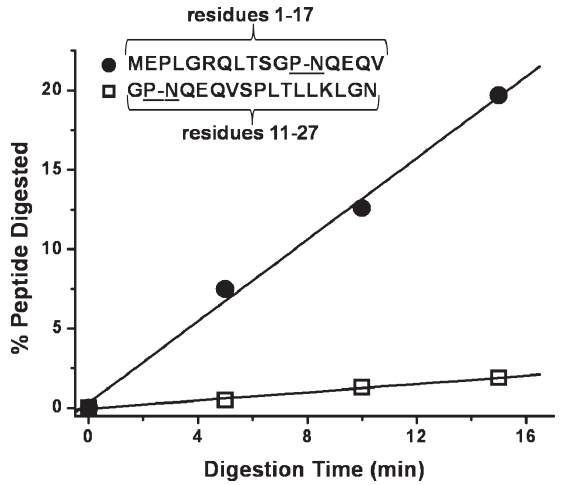

FIGURE 1: Endopeptidase specificity of APCE. Two synthetic peptides representing Met-α_2AP(R6) were digested with equivalent amounts of APCE. The peptide MEPLGRQLTSG**P-N**QEQV (●) contained N-terminal amino acids 1−17 of Met-α_2AP(R6) and served as the endopeptidase substrate. The peptide G**P-N**QEQVSPLTLLKLGN (□) contained amino acids 11−27 in the Met-α_2AP sequence and was used as the substrate for aminodipeptidase cleavage. **P-N** represents the APCE-cleavage site. The substrates and products were quantitated by LC/MS to obtain the percent digestion of each peptide with time.

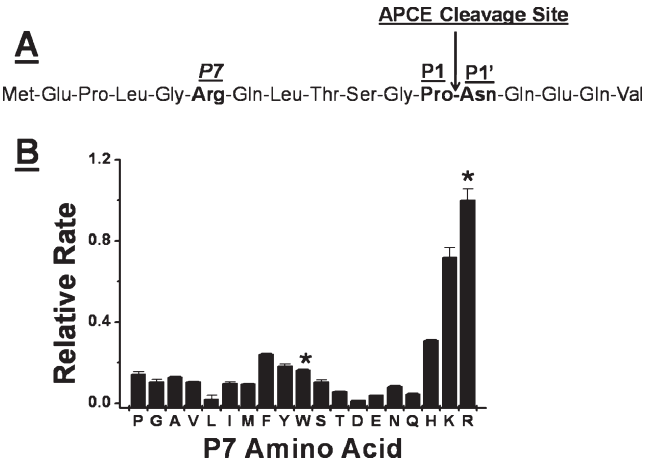

FIGURE 2: APCE residue preference in position P7. (A) A library of the N-terminal peptide containing residues 1−17 of Met-α_2AP(R6) was synthesized to contain each of the native amino acids, less cysteine, as a substitution in P7. (B) Comparison of hydrolysis rates for each peptide with the respective amino acid at P7 is shown on the abscissa. The native P7 polymorphic amino acids, R and W, are labeled (*).

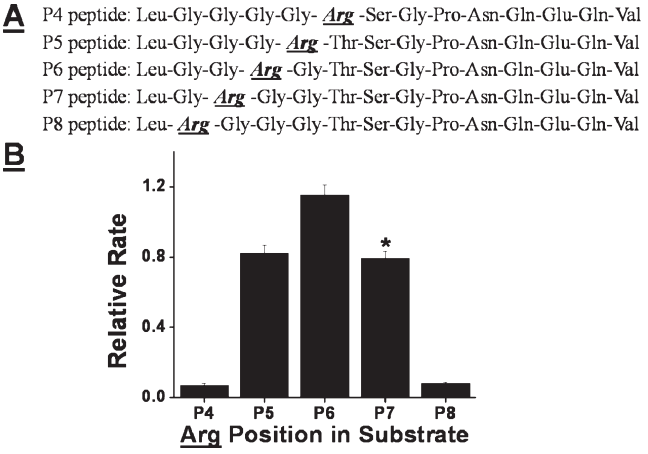

FIGURE 3: APCE-preferred position of Arg relative to the Pro-Asn scissile bond. (A) The panel of peptides examined for APCE-catalyzed hydrolysis: each peptide contained Arg in the P4, P5, P6, P7, or P8 positions and a Gly in the other variable positions. (B) Comparison of hydrolysis rates for each peptide with Arg in position P4, P5, P6, P7, or P8 as shown on the abscissa. The peptide with Arg in its native P7 position is labeled (*). All rates are relative to the hydrolysis rate of the internal standard peptide.

Z-Gly-Pro-AMC as opposed to Gly-Pro-AMC, we found the k_{cat}/K_m of APCE toward GP-AMC to be 6−51-fold lower than the other three substrates, none of which were cleaved by DPPIV; however, k_{cat}/K_m of DPPIV toward GP-AMC was ~30-fold higher than that of APCE (Table 1).

Effect of the P7 Residue on APCE Substrate Specificity. Given the functional R6W polymorphism in Met-α_2AP, we used LC/MS analyses to screen a peptide library containing 19 different amino acids to define the preferred residue in P7. The relative cleavage rates of the synthetic peptides were determined from a library that spanned the Pro^{12}-Asn^{13} cleavage bond (Figure 2A). APCE exhibited a preference for peptide substrates that contained Arg or Lys in P7, both of which have positively charged, basic side chains at neutral pH (Figure 2B). Arg was clearly the optimal P7 amino acid, the peptide containing it being cleaved ~5−10-fold faster than peptides with other amino acids in P7, except for Lys, which was ~70% of the Arg rate (Figure 2B).

To determine if the distance of Arg relative to the Pro^{12}-Asn^{13} scissile bond is important, five similar peptides, each with Arg as a substitution in P4, P5, P6, P7, or P8 and Gly in the other four positions, but otherwise having native residues in the remainder of the N-terminal sequence (residues 4−17) of Met-α_2AP(R6), were digested by APCE and cleavage rates followed by LC/MS analysis (Figure 3A). Each reaction solution contained one experimental peptide (Figure 3A) and internal standard peptide (FRQLTSGPNQEQV). Based on relative cleavage rates, the peptide containing Arg in P6 proved to be the best substrate for APCE, but enhanced rates were also observed with Arg in P7 (native) or P5. Notably slower cleavage rates were observed when Arg occupied position P4 or P8 (Figure 3B).

APCE Substrate Preferences toward P4−P4′ Residue Peptides. APCE cleavage rates of peptide substrates in the P1−P4 sublibraries were determined by LC/MS analysis (Figure 4A). As expected, P1 required Pro while Gly in P2 was an absolute requirement for cleavage by APCE. Both Pro in P1 and Gly in P2 are native in Met-α_2AP. These data are in agreement with our preliminary report (*23*) and those for recombinant FAP utilizing a totally different approach (*24*). In P3, we found Gly to be the most preferred residue, although Ser was reported for recombinant FAP despite Gly not being included in peptides assayed for recombinant FAP specificity (*24*). With respect to P4, APCE exhibited less specificity. Small amino acids such as Gly or Ala in P3 and a number of amino acids in P4 were slightly better than native Ser and Thr, respectively.

P1′−P4′ substrate specificity was analyzed by MALDI-TOF MS, given its speed and cost per experiment (Figure 4B). Only Ser was better than the native Asn in P1′, but seven different amino acids, namely, Trp, Phe, Pro, Tyr, His, Gly, or Ala, were preferred over native Gln at P2′. Negatively charged amino acids were preferred in P3′ as reflected by native Glu and Asp being interchangeable. Finally, native Gln in P4′ was not particularly favored over other amino acids. In fact, the preferred amino acids

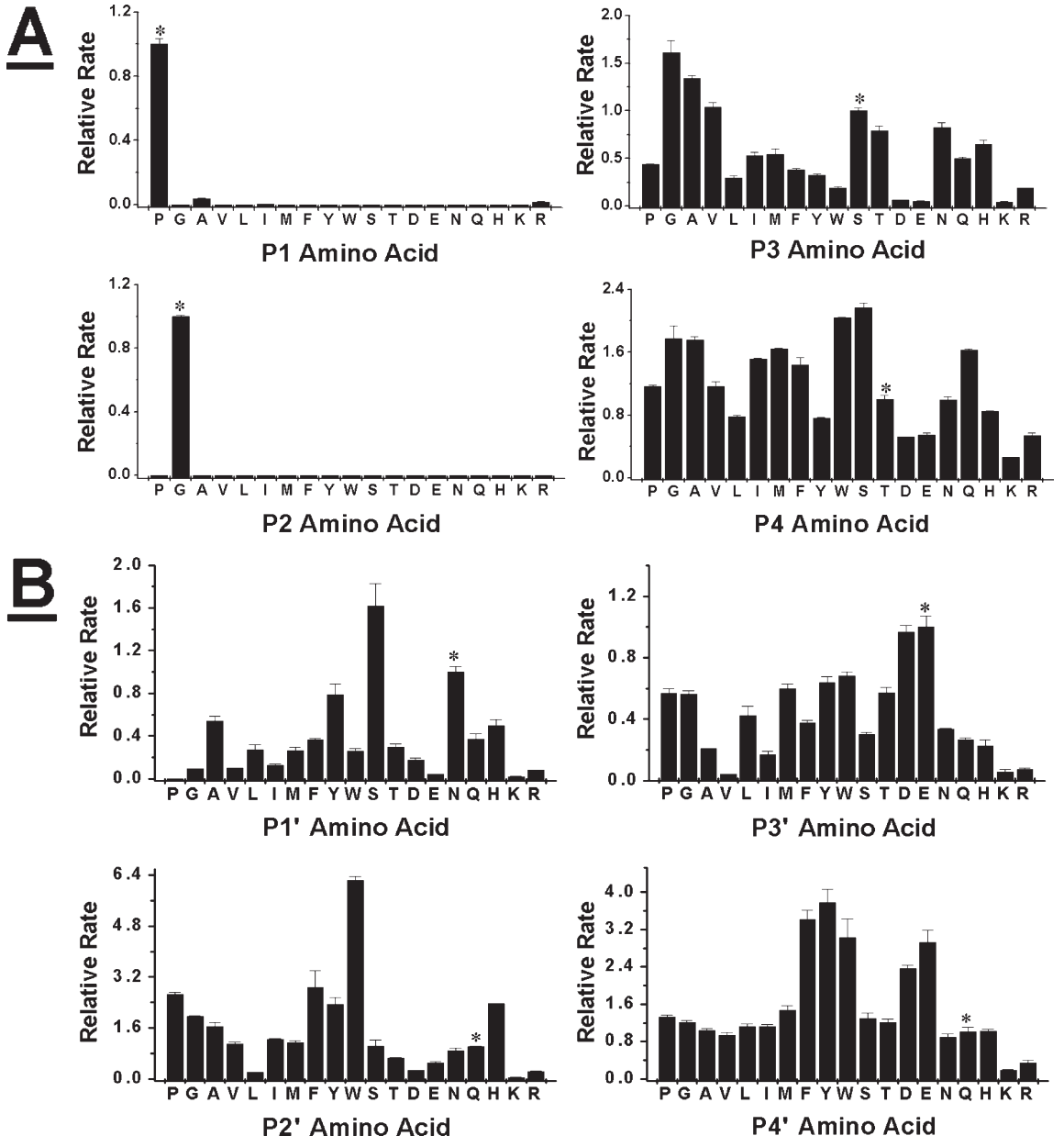

FIGURE 4: APCE peptide substrate preferences for single residue substitutions in P4−P4′. Peptide libraries derived from the P4−P4′ amino acid sequence (TSGP-NQEQ) of Met-α_2AP were synthesized. There were 152 peptides consisting of the common amino acids, less cysteine, which were substituted one at a time in each of the positions P4 through P4′. Peptides were then assayed for relative cleavage rates. The amino acids native to Met-α_2AP are labeled (*). (A) LC/MS analysis of P1−P4 substrate specificity. Peptide libraries representing residues 6 through 17 (FRQL**TSGP**-NQEQV) of Met-α_2AP(R6) were incubated with APCE; each bold letter represents the amino acid subjected to substitution. (B) MALDI-TOF MS analysis of P1′−P4′ substrate specificity. Peptide libraries representing residues 9 through 18 (ATSGP-**NQEQ**VSFR) of Met-α_2AP were incubated with APCE; each bold letter represents a varied amino acid.

in P4′ were aromatic residues, Phe, Tyr, and Trp. In general, APCE manifested tight amino acid specificity in P1 and P2, but P3, P4, and P1′−P4′ tolerated a number of different residues. Notably, neither Lys nor Arg was tolerated in any position of P4−P4′.

In a similar, but not identical study, Edosada et al. (*24*) used recombinant FAP to cleave peptides containing 11 amino acid substitutions spanning P4 through P2′ and found very tight specificity for Pro and Gly at P1 and P2, respectively. Our present study, in which 19 amino acid substitutions were used, showed broad tolerance for residues in P3, P4, P1′, and P2′ of APCE. Both the findings of Edosada et al. (*24*) and our results reported here showed that small neutral amino acids seemed to be preferred in P3. Interestingly, P2′ trended toward aromatic or small neutral amino acids. We included additional substitutions in P3′ and P4′ and found that negatively charged residues appear important in P3′ and that occupancy by Lys, Arg, and His significantly decreases cleavage rates. P4′ definitely preferred aromatic or negatively charged residues. Hence, on compiling results from both studies, there is clear agreement for the strict requirement for Pro and Gly in P2 and P1, whereas a fair amount of hydrophobicity and negativity are favored in the P1′−P4′ sequence. Notably, throughout the P4−P4′ peptide, positively charged residues are the least favored.

Implications of P2 Gly and P7 Arg on APCE inhibition. Besides the Pro^{12}-Asn^{13} scissile bond of Met-α_2AP(R6), both P2 Gly and P7 Arg residues are important for directing APCE substrate specificity (Figures 2 and 4A). Based on the N-terminal

Table 2: Inhibition Constants of APCE Inhibitors

Inhibitor	Structure[a]	*P1*[b]	K_i (μM)[c]
(1) FRQLTSG-pipecolinyl-NQEQV	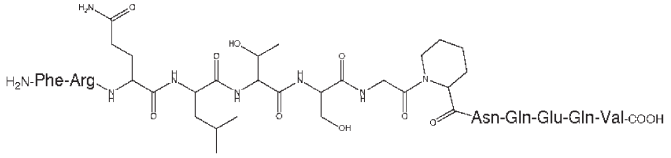		14.0±0.8
(2) FR-*peg*-G-pipecolinyl-NQEQV	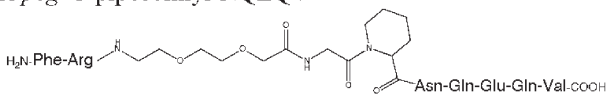		14.8±1.4
(3) FG-*peg*-G-pipecolinyl-NQEQV	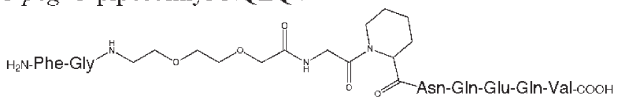		57.1±3.1
(4) FR-*peg*-G-pipecolinyl-NQGQV	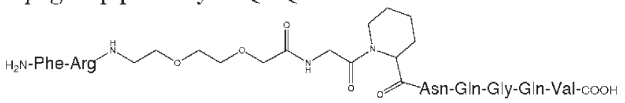		14.5±0.6
(5) FR-*peg*-G-pyrrolidide	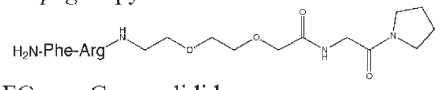		67.7±5.8
(6) FG-*peg*-G-pyrrolidide	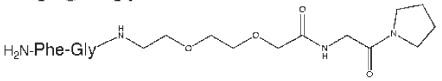		703±68
(7) FR-*peg*-pyrrolidide	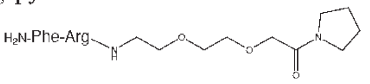		>1000
(8) FR-*peg*-G-[*r*]-fluoropyrrolidide	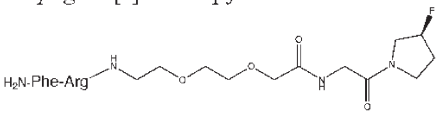		53.8±4.9
(9) FR-*peg*-G-[*s*]-fluoropyrrolidide	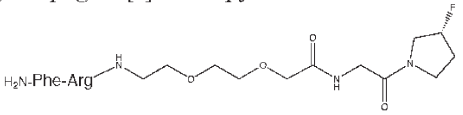		55.3±5.3
(10) FR-*peg*-G-piperidide	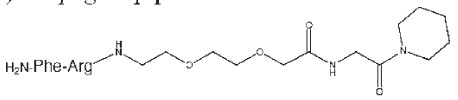		264±23
(11) FR-*peg*-G-pipecolinamide	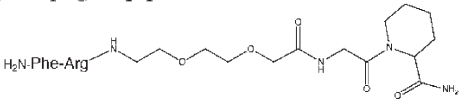		>1000

[a] peg represents a polyethylene glycol derivative, 8-amino-3,6-dioxaoctanoic acid, and [*r*] and [*s*] indicate different stereo configurations. [b] P1 positions are vertically aligned. [c] Data represent the best-fit value ± the standard error.

sequence of Met-α_2AP(R6), inhibitor **1**, FRQLTSG-pipecolinyl-NQEQV, in which P1 Pro was replaced with pipecolinic acid, manifested significant inhibitory activity, having a K_i = 14.0 ± 0.8 μM (Table 2). Inhibitor **2** contained peg (a polyethylene glycol, i.e., 8-amino-3,6-dioxaoctanoic acid) instead of the QLTS residues of inhibitor **1**. Although slightly shorter in linear length than QLTS, lower in molecular weight, and higher in aqueous solubility, inhibitor **2** had about the same K_i value as inhibitor **1**. When P7 Arg in inhibitor **2** was replaced with Gly to form inhibitor **3**, the K_i was reduced ~4-fold, which agrees with our peptide cleavage data showing preference for Arg over Gly in this position (Figure 2). To test the hypothesis that inhibitor **2** may exist in cyclic form as a consequence of the positively charged P7 Arg interacting with negatively charged preferred P3′ Glu, the latter was replaced with Gly to yield inhibitor **4**, which showed about the same inhibitory potency as inhibitor **2**. Hence, P7 Arg in inhibitor **2** must interact directly with APCE and not form a cyclic peptide via an intramolecular charge interaction. This

interpretation was further supported by the comparison of inhibitors **5** with **6**, which showed that inhibitor **5** has about a 10-fold greater potency.

Efforts were undertaken to improve inhibitor **5**, which has pyrrolidine as a Pro-mimetic at P1. First, since fluorinated inhibitors of DPPIV are reported to show remarkable improvements in potency and pharmacokinetics (*25*), inhibitor **5** was fluorinated on the 3-position of the pyrrolidine ring to give either *R* or *S* sterospecificity and termed inhibitor **8** or **9**, respectively. Both were only ~1.3-fold more potent than the nonfluorinated parent, inhibitor **5**. Second, the smaller inhibitor **7** was made by deleting Gly from inhibitor **5**. This was done in an effort to reduce the molecular size of the inhibitor and to determine whether the structurally analogous ethylene glycol unit might substitute for the P2 Gly. Inhibitor **5**, however, showed a >14-fold potency over inhibitor **7**, indicating that P2 Gly is essential for inhibition. Finally, the five-membered ring structure, pyrrolidine, of inhibitor **5** was replaced by a six-membered ring structure, piperidine, to give inhibitor **10**, which was ~4-fold weaker in inhibitory potency than the pyrrolidine-containing construct. Inhibitor **11**, which is inhibitor **10** with a carboxyamide group in its piperidine ring, was less effective than inhibitor **10**.

Inhibition of APCE-Mediated Met-α_2AP Cleavage. Five inhibitors from Table 2 were selected to test their ability to inhibit hydrolysis of the physiologic substrate Met-α_2AP. Inhibition constants shown in Table 2 were determined from 20 min incubations of APCE with the fluorogenic synthetic substrate, Z-Gly-Pro-AMC. Met-α_2AP(R6) was incubated with APCE in a 7 h assay (Figure 5) to compare inhibitors **5** and **6** for the effect of Arg versus Gly in P7 on substrate binding to APCE. Inhibitor **8** was selected because it was the best among the group without P′ sites for inhibiting Z-GlyPro-AMC cleavage, and inhibitor **2** served to represent those with P′ sites. Inhibitor **11** served as a negative control, since it lacked inhibitory properties. When using Met-α_2AP(R6) as substrate (Figure 5), percent inhibition of each inhibitor correlated with the constants listed in Table 2, except for inhibitor **2**. During a 1 h incubation, ~6% of inhibitor **2** was cleaved by APCE to yield two derivatives as detected by LC/MS, (i) FR-peg-G-pipecolinic acid and (ii) NQEQV, neither of which appeared to have any inhibitory effect on APCE. These data imply that it may be possible to develop a substrate analogue into an efficient inhibitor of APCE, which is not cleaved at all or, in worst case, cleaved very slowly (*26*). Since the potency of inhibitor **8** was maintained over 7 h of incubation with APCE (Figure 5B), its IC_{50} value was determined by two different methods: LC/MS to quantify the N-terminal peptide cleaved from Met-α_2AP(R6) by APCE (Figure 6A1) and immunoblot analysis to quantify the amount of intact Met-α_2AP(R6) that remained after exposure to cleavage by APCE (Figure 6B1). LC/MS data were closely fitted to a sigmoidal curve model and yielded an IC_{50} of 91 ± 1.2 μM (Figure 6A2). Using immunoblot data, the IC_{50} could be graphically estimated as ~120 μM (Figure 6B2). While the LC/MS technique is a more useful and accurate approach for determining IC_{50}, the two values obtained by very different methods were in general agreement.

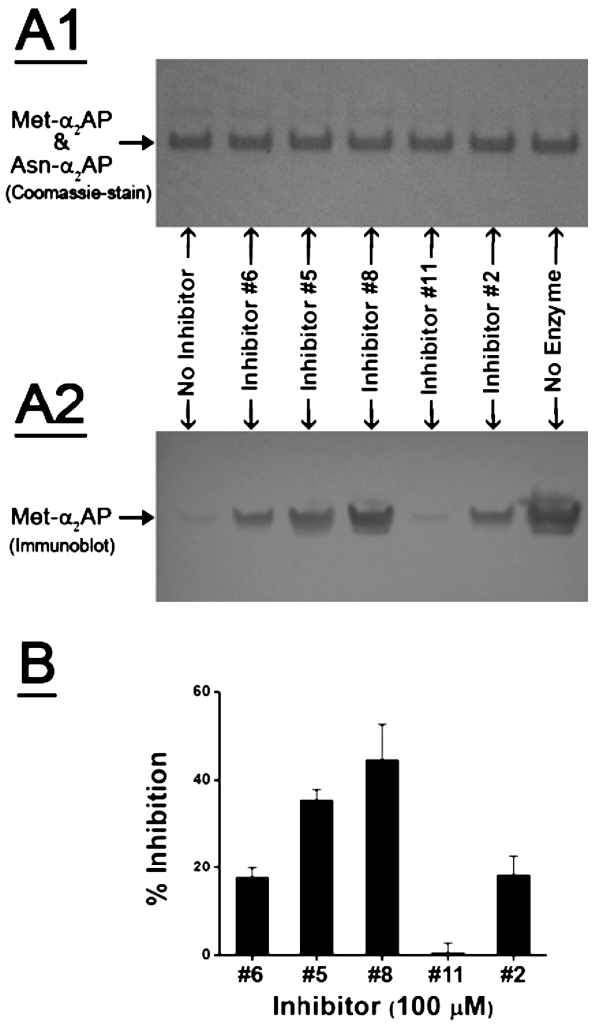

FIGURE 5: Inhibition of Met-α_2AP cleavage by APCE. Met-α_2AP (R6) was incubated for 7 h with APCE and each of the following inhibitors: **2**, **5**, **6**, **8**, or **11**. Controls are indicated as either "no inhibitor" or "no enzyme" when either was omitted. (A1) Coomassie-stained reduced SDS−PAGE analyses and (A2) a representative immunoblot detected by an antibody specific for the N-terminal peptide of Met-α_2AP(R6) that does not react with Asn-α_2AP. (B) Densitometric analysis of immunoblot (A2) for % inhibition of Met-α_2AP(R6) cleavage by each inhibitor. The % inhibition was expressed as [(densitometric value for inhibitor − densitometric value for "no inhibitor")/(densitometric value for "no enzyme" − densitometric value for "no inhibitor")] × 100. Each bar represents the mean ± SE of five experiments.

DISCUSSION

Inhibition of circulating APCE could well raise the plasma level of Met-α_2AP to cause increased endogenous fibrinolytic activity where tendency to thrombosis exists. The membrane location of FAP and the fact that its expression appears restricted to activated stromal fibroblasts of selected cancers and, in some cases, neoplastic parenchymal cells make it an attractive target for inhibitors that restrict proteolytic invasion of extracellular matrix (ECM). Experimental treatment considerations of metastatic cancer raised the possibility that Val-boroPro, a prolyl boronic acid, may be useful for inhibiting FAP and, as a consequence, cancer growth (*8*−*17*). Unfortunately, however, Val-boroPro also inhibited certain dipeptidyl peptidases such as DPPIV and upregulated cytokine and chemokine activities (*27*). Several other prolyl boronic acids have been developed and reported as putative selective inhibitors for FAP (*28*, *29*), but their instability in aqueous buffers and physiologic systems due to reactive electrophiles within their structures have complicated progress (*30*, *31*). Clearly, the development of an effective inhibitor of APCE/FAP may have therapeutic potential for (i) increasing endogenous fibrinolysis in prothrombotic states and (ii) abrogating the expansion of epithelial-derived malignancies.

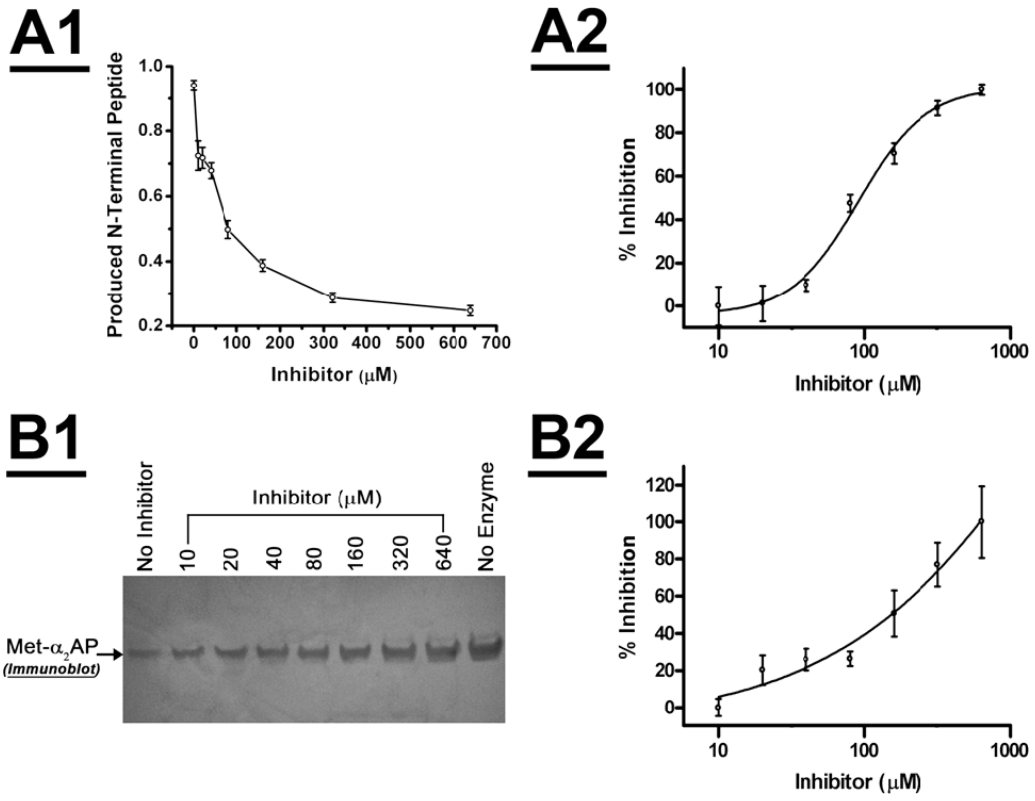

FIGURE 6: Determination of IC_{50} for FR-peg-G-(*R*)-fluoropyrrolidide (inhibitor **8**). After incubating Met-α_2AP(R6) with APCE and inhibitor **8** for 6 h, the reaction mixture was divided for LC/MS analysis of the N-terminal peptide produced from cleavage of Met-α_2AP(R6) and the other half for immunoblot analysis of intact Met-α_2AP(R6). (A1) LC/MS determination of produced N-terminal peptide (PNP) from Met-α_2AP(R6) was expressed as the ratio of sum of area of the N-terminal peptide to sum of area of the internal standard peptide obtained from LC/MS data and then plotted as a function of inhibitor concentration. Each data point is the mean ± SE of three determinations. (A2) For determining an IC_{50}, % inhibition was calculated as [(PNP value for 0 μM inhibitor in panel A1 − PNP value for each concentration of inhibitor)/PNP value for 0 μM inhibitor] × 100. Then the sigmoidal dose−response curve-fit model in Graphpad Prism software was normalized by defining 0% and 100% as the smallest and highest values for each of the % inhibition data sets, respectively. (B1) A representative immunoblot for Met-α_2AP(R6) detection at various inhibitor concentrations by an antibody specific for the N-terminal peptide of Met-α_2AP(R6). (B2) Percent inhibition was calculated as described in the legend to Figure 5B, and curve fitting of normalized % inhibition was performed as described in (A2). Each data point is the mean ± SE of three experiments.

Given that APCE and FAP are essentially identical, we asked the following questions in efforts to analogize inhibitor development to the peptide structure of a native substrate, Met-α_2AP: (i) Does APCE bind to the N-terminal peptide of Met-α_2AP(R6) with greater affinity than that of Met-α_2AP(W6)? (ii) Is Arg6, which is also P7 in the peptide substrate, the most preferred residue in this position for APCE substrate specificity? (iii) In Met-α_2AP(R6) sequence, are the native residues Thr, Ser, Gly, Pro, Asn, Gln, Glu, and Gln in P4, P3, P2, P1, P1′, P2′, P3′, and P4′ positions, respectively, optimal, or even essential for APCE substrate specificity? (iv) Would the sum of these results suggest a peptide template for construction of a specific inhibitor of APCE? (v) And finally, would such an inhibitor block cleavage of Met-α_2AP as well as synthetic substrates?

We first examined endo- and dipeptidase activities of APCE, using extended peptide sequences around the P1−P1′ scissile bond in its only definitive physiologic substrate to date, namely, MEPLGRDQLTSGP-NQEQV and GP-NQEQVSPLTLLKLGN of Met-α_2AP. Given binding considerations, we thought it important to present the enzyme with as much native primary structure as possible on either side of the P1−P1′ bond; however, obviously no peptide extension beyond P2 was feasible in analyses of dipeptidase function. APCE manifests ~10-fold more endopeptidase than dipeptidyl peptidase activity (Figure 1). Based on k_{cat}/K_m values in Table 1, APCE possessed only about 3% of the dipeptidyl peptidase activity of DPPIV. Our findings here are in keeping with those of Aertgeerts et al. (*22*), who used sensitive synthetic fluorogenic dipeptide substrates to show lower recombinant human FAP dipeptidase than endopeptidase activity; however, Collins et al. (*32*) did not detect dipeptidase activity using a bovine serum form of APCE/FAP for cleaving synthetic Gly-Pro-AMC substrate but did characterize endopeptidase activity using Z-Gly-Pro-AMC.

We reasoned that any inhibitor made to mimic the favored Met-α_2AP(R6) substrate cleavage site might involve P4−P4′ positions as well as P7, given the functional impact of the R6W polymorphism in this position. APCE cleavage of substrates from the peptide library definitively established that P1 and P2 absolutely require Pro and Gly, respectively. Virtually any noncharged amino acid could occupy P3 and P4 without major effect on cleavage rate (Figure 4). P7 strongly prefers a positively charged amino acid such as Arg > Lys > His (Figure 2). Because of the striking effect of a positive charge in P7, we posited that the distance from it and the P1−P1′ scissile bond may be a significant factor in specificity of APCE. Hence, P7 Arg was shuffled to P4, P5, P6, or P8, with results showing that Arg in P6 gives faster cleavage rate than Arg in native P7 (Figure 3). While Arg in P5 was about as effective as in native P7, cleavage rates decreased substantially with Arg in P4 or P8. Our results are in keeping with the recent observations of Aggarwal et al. (*33*) that degraded type I collagen is cleaved preferentially at -Gly-Pro-Xaa bonds that have a positively charged Arg or Lys in the P6 site. Likewise, our

findings with P7 Arg are consistent with "electrostatic steering" or "ionic tethering" (*33*−*36*), the latter occurring between a positively charged residue in P7 and an unidentified negatively charged site in close relationship with the active site containing pore of FAP. Certainly this could increase the rate of complex formation and key the substrate's scissile bond to the active site serine within the enzyme. Figure 7 shows our model of the N-terminal peptide of Met-α_2AP(R6) within the recombinant FAP crystallographic structure derived by Aertgeerts et al. (*22*). The pore around the catalytic triad in the structure of FAP is large and can accommodate long peptides. Docking of the 17-mer peptide into this pocket shows that most residues, except the ones at P2, P1, P1′, and P2′, can have different conformations and make contacts with different residues of the enzyme. Arg, at a distance equivalent to 6−7 residues from the scissile bond toward the N-terminus, can be aligned with any of the four different patches of negative charge on the surface of the pore. These interactions can serve as a tether for directing the scissile bond of a substrate to the catalytic site of APCE/FAP.

We determined the residue preferences by initial hydrolysis rates of peptide substrate mixtures from a synthesized peptide library, and while more efficient and cost-effective compared to using individual peptides, the determination of APCE substrate preference could only be expressed as relative k_{cat}/K_m and not as individual K_m values because of competition among the several peptide substrates (*37*). Three fluorogenic peptides modeled on the native N-terminal region sequence of Met-α_2AP were synthesized: MEPLG**R**QLTSGP-AMC, MEPLG**W**QLTSGP-AMC, and GP-AMC. K_m values for the three were 0.021, 0.070, and 0.455 mM, demonstrating that, besides P1 Pro and P2 Gly, an extended sequence N-terminal to the scissile bond, most likely dominated by Arg in P7, clearly confers tighter substrate binding to APCE. Moreover, the correlation of K_m values with residue preference suggests the utility of both approaches for inhibitor development.

Based on the above data, FRQLTSG-pipecolinyl-NQEQV (inhibitor **1**) was synthesized with F added to enhance reverse-phase chromatographic separation. The native sequences, RQLTS and NQEQV, with R in P7, were placed in correct relationship to both G, the required P2 residue, and to P1, which in this case is pipecolinic acid with a six-membered ring instead of five as in Pro. When inhibitor **1** was compared to FR-peg-G-pipecolinyl-NQEQV (inhibitor **2**), both manifested essentially identical K_i values (Table 2), and both were slowly hydrolyzed during lengthy incubations with APCE. The substitution of a peg with a length closely similar to the sum of the omitted residues was done because of its smaller mass, potentially lower antigenicity, and higher aqueous solubility. Since the peptide library data suggested that the P′ residues may not be a critical requirement, noncleavable peptide analogue inhibitors such as FR-peg-G-pyrrolidide (inhibitor **5**), FR-peg-G-[*r*]-flurrroropyrrolidide (inhibitor **8**), and FR-peg-G-piperidide (inhibitor **10**) were synthesized. Inhibitor **2** (K_i = 14 μM) was more potent than inhibitor **8** (K_i = 54 μM) during short incubations with Z-Gly-Pro-AMC, but in ~20-fold longer incubations, where Met-α_2AP(R6) served as the physiologic substrate, inhibitor **8** demonstrated superior activity (Figure 5). The loss of potency with time of inhibitor **2** is explained by slow cleavage of its P1−P1′, i.e., the pipecolinyl−Asn bond. Inhibitor **8** blocked APCE cleavage of Met-α_2AP(R6) in a concentration-dependent manner with an IC_{50} value of 91 μM. Inhibitor **8** was significantly more selective for APCE than DPPIV, the most closely related enzyme to FAP

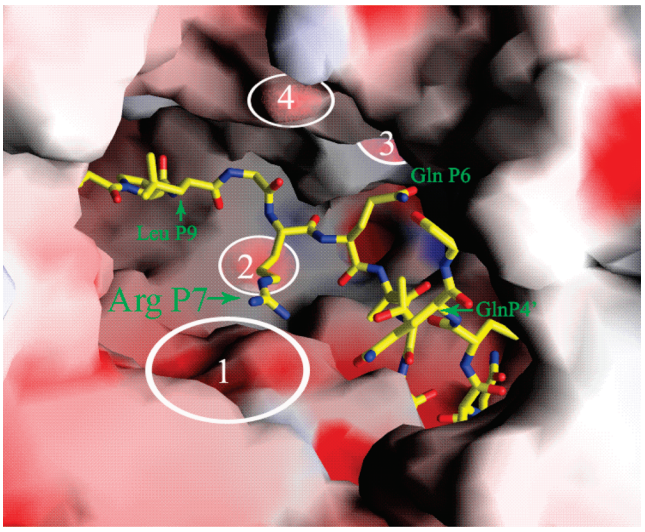

FIGURE 7: Docking of the 17-mer N-terminal peptide of Met-α_2AP (R6) into the FAP active site. Each of the two monomeric units of FAP contains a large pore that can easily dock long peptides in which residues except at P2, P1, P1′, and P2′ can have different conformations and make contacts with different residues of the enzyme. With Arg at a 6−7 residue distance from P1, toward the N-terminus, the surface of the pore is lined with four different patches of negative charge; in particular, main chain oxygen atoms of Leu^{206} and Ala^{207} and hydroxyl groups of Thr^{208}, Tyr^{124}, and Tyr^{210} form one patch, the carbonyl group of Val^{352} with hydroxyl groups of Ser^{353} and Thr^{354} form the second patch; side chains of Tyr^{54} and Tyr^{467} form the third patch; and the carbonyl group of Ala^{452} with the hydroxyl group of Thr^{453} forms the fourth one. Such an arrangement will definitely favor an Arg or Lys residue at the P6 or P7 position. In the model of our 17-mer peptide, the distal guanidinium group of Arg at P7 interacts with the main chain oxygen atom of Ala^{207} and the hydroxyl group of Tyr^{124}. These interactions could serve as a lure for capturing a substrate from solution and directing its scissile bond to the active site of the enzyme.

(48% amino acid sequence identity) in the clade of prolyl-specific serine proteinases (*6*), as even up to 2 mM did not inhibit DPPIV. DPPIV does not cleave Z-Gly-Pro-AMC or Met-α_2AP(R6), but it does readily cleave the dipeptidyl substrate, Gly-Pro-AMC. Acetyl-Gly-boroPro and acetyl-Gly-Pro-nitrile have been reported as more potent for inhibiting FAP, but with a fairly narrow concentration window for also inhibiting DPPIV, with acetyl-Gly-boroPro having K_i values of 23 nM for FAP and 377 nM for DPPIV, and acetyl-Gly-Pro-nitrile with K_i values of 6.8 and 61 μM for the two enzymes, respectively (*7*). We propose that the higher selectivity of inhibitor **8** for APCE with a K_i of 54 μM, and no inhibition of DPPIV even at 2 mM, suggests that a peptide motif modeled on Arg-xxx-Gly-Pro, where xxx represents a linker of ~2−4 amino acids in length, may be useful for APCE/FAP-specific inhibitor design and avoidance of -boroPro "warhead" inhibitors because of their potent electrophilic properties, broad specificities, and consequent toxicity (*31*).

ACKNOWLEDGMENT

We thank Chung S. Lee and Jin G. Chun for technical assistance.

REFERENCES

1. Lee, K. N., Jackson, K. W., Christiansen, V. J., Chung, K. H., and McKee, P. A. (2004) A novel plasma proteinase potentiates α_2-antiplasmin inhibition of fibrin digestion. *Blood 103*, 3783–3788.

2. Christiansen, V. J., Jackson, K. W., Lee, K. N., and McKee, P. A. (2007) The effect of a single nucleotide polymorphism on human α_2-antiplasmin activity. *Blood 109*, 5286–5292.
3. Lee, K. N., Jackson, K. W., Christiansen, V. J., Lee, C. S., Chun, J. G., and McKee, P. A. (2007) Why α_2-antiplasmin must be converted to a derivative form for optimal function. *J. Thromb. Haemostasis 5*, 2095–2104.
4. Lee, K. N., Jackson, K. W., Christiansen, V. J., Lee, C. S., Chun, J. G., and McKee, P. A. (2006) Antiplasmin-cleaving enzyme is a soluble form of fibroblast activation protein. *Blood 107*, 1397–1404.
5. Goldstein, L. A., Ghersi, G., Pineiro-Sanchez, M. L., Salamone, M., Yeh, Y., Flessate, D., and Chen, W. T. (1997) Molecular cloning of seprase: a serine integral membrane protease from human melanoma. *Biochim. Biophys. Acta 1361*, 11–19.
6. Scanlan, M. J., Raj, B. K., Calvo, B., Garin-Chesa, P., Sanz-Moncasi, M. P., Healey, J. H., Old, L. J., and Rettig, W. J. (1994) Molecular cloning of fibroblast activation protein alpha, a member of the serine protease family selectively expressed in stromal fibroblasts of epithelial cancers. *Proc. Natl. Acad. Sci. U.S.A. 91*, 5657–5661.
7. Meadows, S. A., Edosada, C. Y., Mayeda, M., Tran, T., Quan, C., Raab, H., Wiesmann, C., and Wolf, B. B. (2007) Ala^{657} and conserved active site residues promote fibroblast activation protein endopeptidase activity via distinct mechanisms of transition state stabilization. *Biochemistry 46*, 4598–4605.
8. Bhati, R., Patterson, C., Livasy, C. A., Fan, C., Ketelsen, D., Hu, Z., Reynolds, E., Tanner, C., Moore, D. T., Gabrielli, F., Perou, C. M., and Klauber-Demore, N. (2008) Molecular characterization of human breast tumor vascular cells. *Am. J. Pathol. 172*, 1381–1390.
9. Chen, D., Kennedy, A., Wang, J. Y., Zeng, W., Zhao, Q., Pearl, M., Zhang, M., Suo, Z., Nesland, J. M., Qiao, Y., Ng, A. K., Hirashima, N., Yamane, T., Mori, Y., Mitsumata, M., Ghersi, G., and Chen, W. T. (2006) Activation of EDTA-resistant gelatinases in malignant human tumors. *Cancer Res. 66*, 9977–9985.
10. Cohen, S. J., Alpaugh, R. K., Palazzo, I., Meropol, N. J., Rogatko, A., Xu, Z., Hoffman, J. P., Weiner, L. M., and Cheng, J. D. (2008) Fibroblast activation protein and its relationship to clinical outcome in pancreatic adenocarcinoma. *Pancreas 37*, 154–158.
11. Ge, Y., Zhan, F., Barlogie, B., Epstein, J., Shaughnessy, J.Jr., and Yaccoby, S. (2006) Fibroblast activation protein (FAP) is upregulated in myelomatous bone and supports myeloma cell survival. *Br. J. Haematol. 133*, 83–92.
12. Iwasa, S., Jin, X., Okada, K., Mitsumata, M., and Ooi, A. (2003) Increased expression of seprase, a membrane-type serine protease, is associated with lymph node metastasis in human colorectal cancer. *Cancer Lett. 199*, 91–98.
13. Koperek, O., Scheuba, C., Puri, C., Birner, P., Haslinger, C., Rettig, W., Niederle, B., Kaserer, K., and Garin-Chesa, C. P. (2007) Molecular characterization of the desmoplastic tumor stroma in medullary thyroid carcinoma. *Int. J. Oncol. 31*, 59–67.
14. Mori, Y., Kono, K., Matsumoto, Y., Fujii, H., Yamane, T., Mitsumata, M., and Chen, W. T. (2004) The expression of a type II transmembrane serine protease (seprase) in human gastric carcinoma. *Oncology 67*, 411–419.
15. Narra, K., Mullins, S. R., Lee, H. O., Strzemkowski-brun, B., Magalong, K., Christiansen, V. J., Mckee, P. A., Egleston, B., Cohen, S. J., Weiner, L. M., Meropol, N. J., and Cheng, J. D. (2007) Phase II trial of single agent Val-boroPro (talabostat) inhibiting fibroblast activation protein in patients with metastatic colorectal cancer. *Cancer Biol. Ther. 6*, 1691–1699.
16. Okada, K., Chen, W. T., Iwasa, S., Jin, X., Yamane, T., Ooi, A., and Mitsumata, M. (2003) Seprase, a membrane-type serine protease, has different expression patterns in intestinal- and diffuse-type gastric cancer. *Oncology 65*, 363–370.
17. Zhang, M. Z., Qiao, Y. H., Nesland, J. M., Trope, C., Kennedy, A., Chen, W. T., and Suo, Z. H. (2007) Expression of seprase in effusions from patients with epithelial ovarian carcinoma. *Chin. Med. J. (Engl. Ed.) 120*, 663–668.
18. Cheng, J. D., Dunbrack, R. L.Jr., Valianou, M., Rogatko, A., Alpaugh, R. K., and Weiner, L. M. (2002) Promotion of tumor growth by murine fibroblast activation protein, a serine protease, in an animal model. *Cancer Res. 62*, 4767–4772.
19. Wang, X. M., Yu, D. M., Mccaughan, G. W., and Gorrell, M. D. (2005) Fibroblast activation protein increases apoptosis, cell adhesion, and migration by the lx-2 human stellate cell line. *Hepatology 42*, 935–945.
20. Milner, J. M., Kevorkian, L., Young, D. A., Jones, D., Wait, R., Donell, S. T., Barksby, E., Patterson, A. M., Middleton, J., Cravatt, B. F., Clark, I. M., Rowan, A. D., and Cawston, T. E. (2006) Fibroblast activation protein alpha is expressed by chondrocytes following a pro-inflammatory stimulus and is elevated in osteoarthritis. *Arthritis Res. Ther. 8*, R23.
21. Acharya, P. S., Zukas, A., Chandan, V., Katzenstein, A. L., and Pure, E. (2006) Fibroblast activation protein: a serine protease expressed at the remodeling interface in idiopathic pulmonary fibrosis. *Hum. Pathol. 37*, 352–360.
22. Aertgeerts, K., Levin, I., Shi, L., Snell, G. P., Jennings, A., Prasad, G. S., Zhang, Y., Kraus, M. L., Salakian, S., Sridhar, V., Wijnands, R., and Tennant, M. G. (2005) Structural and kinetic analysis of the substrate specificity of human fibroblast activation protein alpha. *J. Biol. Chem. 280*, 19441–19444.
23. Jackson, K. W., Christiansen, V. J., Lee, K. N., and McKee, P. A. (2005) Determination of antiplasmin cleaving enzyme substrate specificity and inhibitor development by peptide library analyses. *FASEB J. 19*, A864.
24. Edosada, C. Y., Quan, C., Tran, T., Pham, V., Wiesmann, C., Fairbrother, W., and Wolf, B. B. (2006) Peptide substrate profiling defines fibroblast activation protein as an endopeptidase of strict Gly (2)-Pro(1)-cleaving specificity. *FEBS Lett. 580*, 1581–1586.
25. Hagmann, W. K. (2008) The many roles for fluorine in medicinal chemistry. *J. Med. Chem. 51*, 4359–4369.
26. Baggio, R., Shi, Y. Q., Wu, Y. Q., and Abeles (1996) From poor substrates to good inhibitors: design of inhibitors for serine and thiol proteases. *Biochemistry 35*, 3351–3353.
27. Cunningham, C. C. (2007) Talabostat. *Expert Opin. Investig. Drugs 16*, 1459–1465.
28. Edosada, C. Y., Quan, C., Wiesmann, C., Tran, T., Sutherlin, D., Reynolds, M., Elliott, J. M., Raab, H., Fairbrother, W., and Wolf, B. B. (2006) Selective inhibition of fibroblast activation protein protease based on dipeptide substrate specificity. *J. Biol. Chem. 281*, 7437–7444.
29. Tran, T., Quan, C., Edosada, C. Y., Mayeda, M., Wiesmann, C., Sutherlin, D., and Wolf, B. B. (2007) Synthesis and structure-activity relationship of N-acyl-gly-, N-acyl-sar- and N-blocked-boroPro inhibitors of FAP, DPP4, and POP. *Bioorg. Med. Chem. Lett. 17*, 1438–1442.
30. Coutts, S. J., Kelly, T. A., Snow, R. J., Kennedy, C. A., Barton, R. W., Adams, J., Krolikowski, D. A., Freeman, D. M., Campbell, S. J., Ksiazek, J. F., and Bachovchin, W. W. (1996) Structure-activity relationships of boronic acid inhibitors of dipeptidyl peptidase IV: variation of the P2 position of Xaa-boroPro dipeptides. *J. Med. Chem. 39*, 2087–2094.
31. Wolf, B. B., Quan, C., Tran, T., Wiesmann, C., and Sutherlin, D. (2008) On the edge of validation—cancer protease fibroblast activation protein. *Mini. Rev. Med. Chem. 8*, 719–727.
32. Collins, P. J., McMahon, G., O'Brien, P., and O'Connor, B. (2004) Purification, identification and characterization of seprase from bovine serum. *Int. J. Biochem. Cell Biol. 36*, 2320–2333.
33. Aggarwal, S., Brennen, W. N., Kole, T. P., Schneider, E., Topaloglu, O., Yates, M., Cotter, R. J., and Denmeade, S. R. (2008) Fibroblast activation protein peptide substrates identified from human collagen I derived gelatin cleavage sites. *Biochemistry 47*, 1076–1086.
34. Myles, T., Le Bonniec, B. F., Betz, A., and Stone, S. R. (2001) Electrostatic steering and ionic tethering in the formation of thrombin-hirudin complexes: the role of the thrombin anion-binding exosite. *Biochemistry 40*, 4972–4979.
35. Wade, R. C., Gabdoulline, R. R., Ludemann, S. K., and Lounnas, V. (1998) Electrostatic steering and ionic tethering in enzyme-ligand binding: insights from simulations. *Proc. Natl. Acad. Sci. U.S.A. 95*, 5942–5949.
36. Cation-pi interaction (2009) *Wikipedia*.
37. Fersht, A. (1985) Enzyme Structure and Mechanism, 2nd ed., Freeman, New York.